A Characterization of 3D Printability

Ioannis Fudos[1], Margarita Ntousia[1], Vasiliki Stamati[1] Paschalis Charalampous[2] Theodora Kontodina[2] Ioannis Kostavelis[2] Dimitrios Tzovaras[2] Leonardo Bilalis[3]

[1] Dept. of Computer Science & Engineering, University of Ioannina, {fudos, mntousia, vstamati}@cse.uoi.gr
[2]Centre for Research and Technology Hellas, Information Technologies Institute, {pcharalampous, kontodinazoli, gkostave, Dimitrios.Tzovaras}@iti.gr
[3]3D Life, leonardo.bilalis@3dlife.gr

Corresponding author: Ioannis Fudos, fudos@cse.uoi.gr

Abstract.

Additive Manufacturing (AM) is currently considered as the spark of a new industrial revolution, due to its versatility in creating 3D structures of unprecedented design freedom and geometric complexity in comparison with conventional manufacturing techniques. Due to differences in AM technologies the final fabricated part can vary, sometimes dramatically, from the originally designed one, therefore raising issues regarding dimensional accuracy, surface finish, mechanical properties, functional and geometrical requirements. Various research efforts have articulated the correlation between AM technologies and design process, in terms of integrating specific design rules or guidelines pertinent to model complexity, design potentials and constraints of each AM process.

In this work we propose a novel approach to assessing the quality and ability of a 3D model to be printed successfully (a.k.a *printability*) on a specific AM machine. This is utilized by taking into consideration the model mesh complexity and certain design features. A *printability score* is derived for a model in reference to a specific 3D printing technology, expressing the probability of obtaining a robust and accurate end result for 3D printing on a specific AM machine. The printability score can be used either to determine which 3D technology is more suitable for manufacturing a specific model or as a guide to redesigning the model to ensure printability. We verify this framework by conducting 3D printing experiments for benchmark models which are printed on three AM machines employing different technologies: Fused Deposition Modeling (FDM), Binder Jetting (3DP), and Material Jetting (Polyjet).

Keywords: Additive manufacturing, 3D printing technologies, printability score
DOI: https://doi.org/10.14733/cadaps.2021.aaa-bbb

© 2021 CAD Solutions, LLC, http://www.cad-journal.net

1 INTRODUCTION

Additive Manufacturing (AM) is currently being promoted as the spark of a new industrial revolution, due to its versatility in creating 3D structures of unprecedented design freedom and geometric complexity in comparison with conventional manufacturing techniques [15, 5]. AM refers to a great variety of commercially available technologies that are most widely applied to manufacture 3D models directly from CAD data, based on successive layer deposition of material in a pre-arranged pattern. Due to differences in AM technologies, in regards to employed processes, machines and materials, the final fabricated part can vary, sometimes dramatically, from the originally designed one, therefore raising issues regarding dimensional accuracy, surface finish, mechanical properties, functional and geometrical requirements [8, 12]. Various research efforts have articulated the correlation between AM technologies and design process, in terms of integrating specific design rules or guidelines pertinent to model complexity, design potentials and constraints of each AM process [17, 16].

In this work we study, determine and correlate the complexity and the design feature properties of a CAD model with its ability to be printed - a.k.a. *printability* - using a specific printing technology. This is accomplished mainly in terms of structural robustness and dimensional accuracy of the corresponding 3D model. We propose a novel approach that, by taking into consideration the model mesh complexity and certain design features, computes a $printability\ score$ for a specific 3D printing technology. This score expresses the probability of a robust and accurate end result for 3D printing on a specific AM machine. To achieve this we isolate feature design rules often used in design guidelines for AM, whose parameter values directly affect the quality of a manufactured model and map them to probability functions that, when evaluated, produce a printability score. This metric can be used either to determine which 3D technology is more suitable for manufacturing a specific model or as a guide to redesigning the model to ensure printability. We verify this measure by conducting printing experiments for several benchmark models as test cases on three AM machines employing different technologies: Fused Deposition Modeling (FDM), Binder Jetting (3DP), and Material Jetting (Polyjet). The proposed framework is not restricted to these 3D printing technologies and can be parameterized and/or extended to estimate printability for other AM technologies.

2 RELATED WORK

3D models, as detailed representations of solids or surfaces, are commonly used in several domains such as medicine, engineering, analysis, manufacturing, arts etc. One critical 'parameter' that affects several functions and processes of these models, such as design, engineering and manufacturing, is the complexity of the model. Despite the fact that there is no standard objective complexity metric, several researchers over the years have followed different approaches to define and measure model complexity mainly for purposes of implementation time and cost reduction. It is also widely accepted that the more complex the model the less robust and flexibly it is. Also a CAD model with high complexity makes it difficult for adjustments, modifications and analysis but also affects production time and cost. That is why it is important to reduce the complexity of a model by suppressing the less significant features and consequently reduce the data describe these features CAD [13, 6, 10].

Even though geometrical and CAD model complexities might be related, they are not the same, since the second one refers to the complexity of the CAD model which is used to represent one component, its features and the relationships between them. Over the years several researchers studied model classification, with Forrest [6] suggesting 3 types of complexity starting with geometrical complexity, referring to basic elements such as points, lines, surfaces, etc. combinatorial complexity, which counts the elements of a model, the number of vertices in a polynomial mesh, edges, faces, etc. and dimensional complexity, which characterizes a model as 2D, 2.5D or 3D.

Other complexity metrics discussed over the years are algebraic, topological, morphological and combinatorial [13]. Algebraic complexity deals with the complexity degree of the polynomials required to represent the exact shape of a model. In CSG (Constructive Solid Geometry) a complex solid or surface object can

© 2021 CAD Solutions, LLC, http://www.cad-journal.net

be created by combining simpler primitive objects such as boxes, cylinders, spheres, pyramids etc. through Boolean operations. Surfaces of CSG primitives are also defined by polynomials. In case of free form/sculptured shapes, a larger amount of quadric primitives is required for a closer approximation since the CSG model is not enough. CSG can also be performed on polygonal meshes, and may or may not be procedural and/or parametric. Topological complexity deals with 3D geometries, such as surfaces, that are not boundaries of a solid, models with internal structure, non-regularized shapes, measures the existence of holes, non-manifold singularities, self-intersections and finally the genus complexity. Morphological complexity deals with the number of the features of a shape, its size, smoothness and regularity. Triangular mesh subdivision can increase its smoothness. Through the subdivision process, high-resolution models are achieved; the number of vertices on the model is increased leading to more rounded curves. Combinatorial complexity also deals with the reducing of the number of vertices in a triangular mesh. By reducing the combinatorial complexity the model might be simpler but also less accurate.

Another approach uses the number of surfaces a component has as complexity metrics; the larger the number, the more complex the model is. The number of the triangles in the STL file used for component representation is another assumption of geometric complexity leading to high quality fabricated parts. Other approaches calculate geometric complexity by comparing the volume of the component with the volume of its bounding box. Both the number and the shape of the features forming a model, affect the geometric complexity since a large number of irregular, thin or even curved features increases not only the computed printing time but also the final form of the fabricated part [10].

The quality of a fabricated part is directly linked to the design principles and rules followed during the design phase, prior to printing. There is a plethora of work that evaluate AM processes and correlates them with design for additive manufacturing(dfAM)[3]. Design rules have been defined for specific 3D printing technologies, to help designers produced parts of high quality and in conformance with the initial design. In [9] a review is provided on design principles that have been defined based on design rules for AM and a Guide-to-Principle-to-Rule (GPR) approach is proposed to assist the design process for better manufacturing. Design rules are grouped together in [7] to form modules as a more dynamic and designer-friendly way of dealing with the design process and a case study is presented on powder bed fusion technology. Design rules for AM were developed in [2] based on geometrical standards and attributes that characterize the object shapes. Three different technologies were used to manufacture the elements for different attribute values and a design catalogue is created. In [18] an analysis of design features in AM is provided and a feature-based approach to orientating parts for optimized building in AM is presented.

The subject of print failure is addressed in [3]. The authors designed and implemented a dfAM worksheet that is used either in the conceptual phase or the CAD phase of the design process. The use of the worksheet led to a decrease in print failures.

Our work focuses on evaluating the printability of a model on a specific 3D printing technology, following the design phase. It does not use design rules to guide the design process, as is more often the case in the aforementioned literature, but uses them as an evaluation guideline to help predict the quality of the 3D print on a certain AM machine and support the decision making. It could, however, be used as knowledge for re-designing of a model to improve the printability on a specific AM machine.

For the purposes of the present work and in order to measure the printability of a model the geometrical complexity will be taken into account regarding the number of triangles in the STL file which affect the regularity and smoothness of the final surface. The volumes of the different triangulated models and the corresponding Bounding Boxes will be compared with the initial CAD model from which the deviation rate will be derived. As for the geometric features of the model, such as the wall thickness, self supporting angles and holes[1], they play a significant role and will be taken into account for the evaluation of printability.

© 2021 CAD Solutions, LLC, http://www.cad-journal.net

3 MODEL AND PART CHARACTERISTICS THAT AFFECT PRINTABILITY

The quality of a 3D printed model, in reference to its robustness and conformance to the initial model, depends on various parameters. In the present work we focus on the 3D representation of the model which is used for printing and specific design characteristics of the model that might affect its printability.

3.1 Geometric Primitives and Benchmarks

For evaluating the 3D design and printing process, we used models of geometric primitives and benchmark models designed especially for this purpose. The geometric primitives included spheres, cylinders, tori and rectangular parallelepipeds, and triangular meshes of different mesh resolutions were created for each primitive. Also, three different benchmarks were designed to test and evaluate different design characteristics, printing capabilities and limits. As shown in Figure 1, the first benchmark (B1) contains thin bridges of different lengths, walls (supported and unsupported), holes of various diameters and various other small details. The second benchmark (B2) has thin parts (thin walls and pin), overhangs of varying angles, whilst the third benchmark (B3) is constructed using basic CSG operations and features one through-hole, supported walls, notches, and bosses.

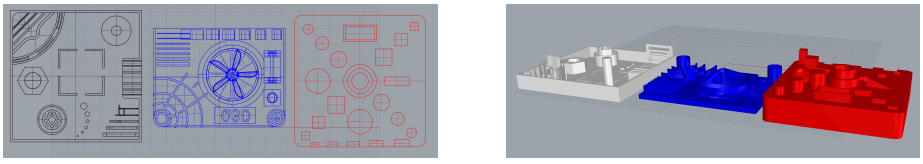

(a) Top view of the benchmark models. (b) Perspective view of the models

Figure 1: Different views of the three benchmark models: B1 (left), B2 (middle), B3 (right)

3.2 Mesh Complexity

In order to measure the printability of the designed CAD models, the geometrical complexity will be measured as the complexity of the mesh representation of the CAD model which is submitted to the AM machine for slicing (and/or *g-code* production) and printing, and therefore referred to as *mesh complexity*. After the design process is complete, the CAD models are exported as polygon meshes, commonly in the form of triangles, and stored in an STL file. We define the mesh complexity C of a CAD model M that is converted to a mesh that consists of a set of triangles *PLG(M)* that approximates the initial CAD model as:

$$C_M = |PLG(M)| \tag{1}$$

If the mesh consists of convex polygons (not necessarily triangles), then each convex polygon p with $v(p)$ vertices is triangulated and the overall mesh complexity is:

$$C_M = \sum_{p \in M} v(p) - 2 \tag{2}$$

For each of the CAD geometric primitives and benchmarks, four triangulations of different resolutions were calculated, starting from a low quality representation to a highest quality almost matching the initial geometry of the models. For each of these triangulations the new volumes and bounding boxes were calculated and the corresponding graphs were plotted to display the deviation between the meshed and the initial CAD model. A Mean Curvature Analysis was performed for all the initial and triangulated models to measure the average

© 2021 CAD Solutions, LLC, http://www.cad-journal.net

value between Minimum and Maximum curvatures and the values of the different curvatures for each vertex are summarized in histograms for a visual representation of the data distribution.

As an example, the models of the sphere, cylinder and B3 benchmark are presented in more detail. The various measurements of the meshed models are illustrated in Tables 1,2 and 3. The resolution of a mesh is directly correlated to the quality, level of detail and robustness of its corresponding printed form. Models approximated by lower resolution meshes produce printed models that exhibit significant deviations from the original model through loss of detail and surface quality reduction. Mesh complexity is also related to the morphology of the model. Surfaces of high curvature must be represented by higher resolution meshes to better approximate the initial CAD model. For instance, the triangulation of a CAD model leading to a representation with 168 faces causes a reduction in the model volume over 8%, which decreases as the number of elements increases. As such, for a model with 148224 faces the percentage of loss asymptotically reaches 0%. The same observations apply to the other models and are visualized in Figures 3, 5 and 7. The same logic applies to the calculation of the new bounding boxes.

Figure 2 shows the Mean Curvature Analysis performed on the initial CAD models which is correlated with the data range of the different curvatures for each meshed model presented in histograms of Figures 4, 6 and 8. More specifically, Figure 4 displays the curvature data distribution of the meshed primitive sphere for four meshes of different resolutions, starting with the lowest one of 168 faces to the highest with 148224 faces. The graph data changes depending on the curvature of each triangle and in the last one it is almost uniform. In Figure 6 the curvature data distribution of the meshed cylinder for the four different mesh resolutions changes for the different areas of the cylinder, with the higher values occurring in the edges of the top and bottom surface. Finally, the curvature data distribution of the meshed B3 benchmark is displayed in Figure 8, with the lowest quality corresponding to 634 faces and the highest to 394682 faces. The final distribution is bimodal, with the two peaks representing the two half spheres of the model. The higher the resolution of the meshed model the lower the deviation with the initial CAD model, leading to better results in the final printed model.

Sphere D: 3 cm - Volume: $1.414e-005$ m3				
Triangular Mesh No of faces	(Volume e-005)m3	BBox (cm) X axis	Y axis	Z axis
168	1.299	3.00	2.92	2.88
1520	1.399	3.00	3.00	3.00
14640	1.412	3.00	3.00	3.00
148224	1.414	3.00	3.00	3.00

Table 1: Geometrical measurements of the sphere primitive

3.3 Design Rules

Another factor that should be considered when discussing printability is the design process. Designing and printing a CAD model are two separate processes which may result in different outcomes in terms of functionality and geometry. The quality and robustness of a 3D printed model are directly correlated to the AM technology used, the materials and parameters selected for printing and the design rules applied during the initial computer aided design phase. There are design rules that conform with AM technologies and design guidelines that should be considered when designing a model for manufacturing with a specific 3D printing technology[4]. For example, if a model has an overhang feature of over 45° and is to be manufactured using FDM technology, then supports must be added to the structure to ensure printing feasibility. However, when

© 2021 CAD Solutions, LLC, http://www.cad-journal.net

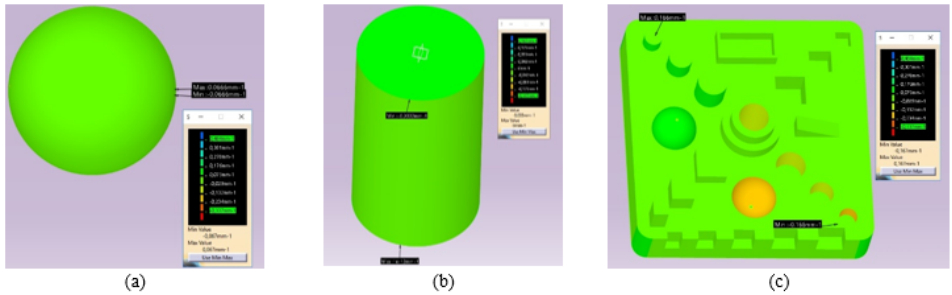

Figure 2: Surface curvature analysis of the initial CAD models (a) sphere (b) cylinder and (c) B3 benchmark

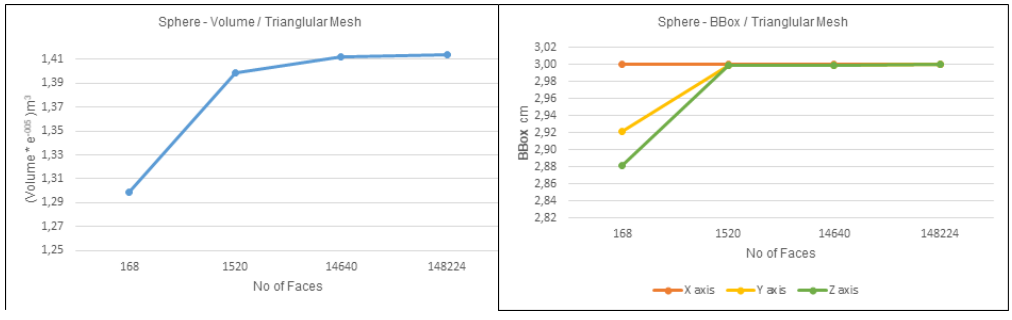

(a) Volume to Triangular mesh diagram (b) BBox to Triangular mesh diagram

Figure 3: Diagrams presenting the effect of triangular mesh over (a) sphere volume and (b) sphere ox

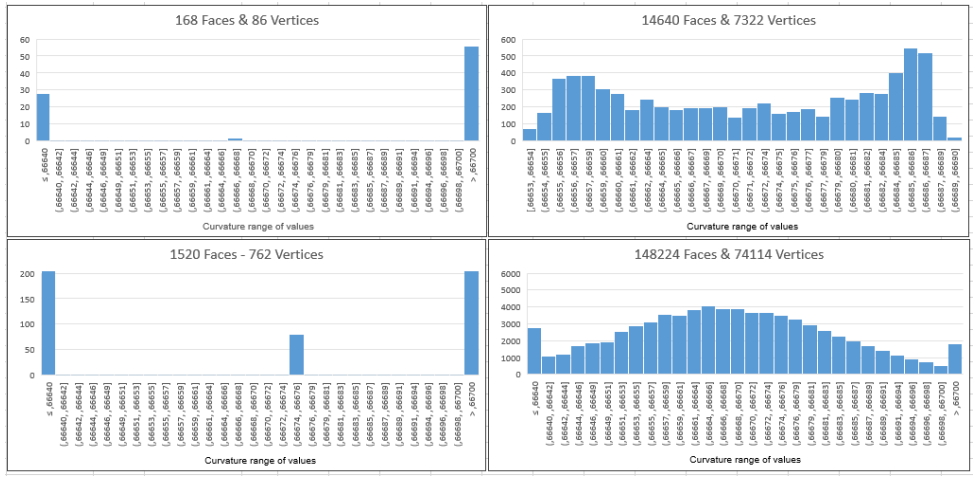

Figure 4: Histograms presenting curvature data distribution of sphere for different triangular meshes

the same model is printed on a powder-bed AM machine support structures are not necessary.

In this work we examine design characteristics and the corresponding design rules that must be enforced for a CAD model to ensure its printability using a specific AM technology. The final printed model depends on

© 2021 CAD Solutions, LLC, http://www.cad-journal.net

Cylinder D: 1.5 cm & H: 5.0 cm - Volume: $3.534e-005$ m3				
Triangular Mesh No of faces	(Volume e-005)m3	Bbox (cm)		
		X axis	Y axis	Z axis
52	3.417	2.93	5.00	3.00
1300	3.520	3.00	5.00	3.00
17372	3.533	3.00	5.00	3.00
94316	3.540	3.00	5.00	3.00

Table 2: Geometrical measurements of the cylinder

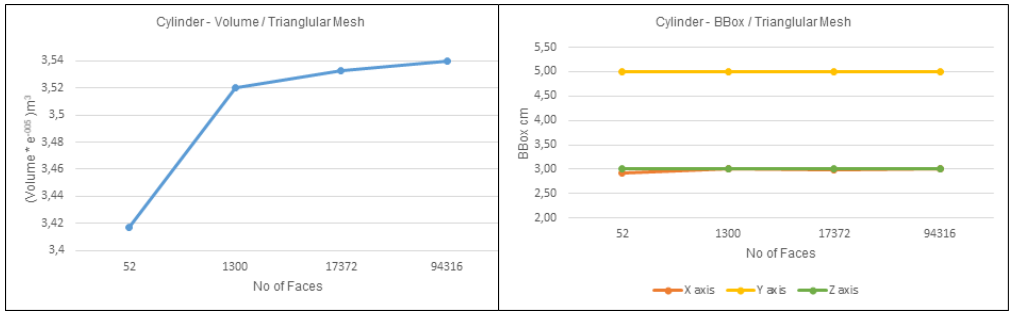

(a) Volume to triangular mesh diagram (b) BBox to Triangular mesh diagram

Figure 5: Diagrams displaying the effect of triangular mesh over (a) cylinder volume and (b) cylinder bbox

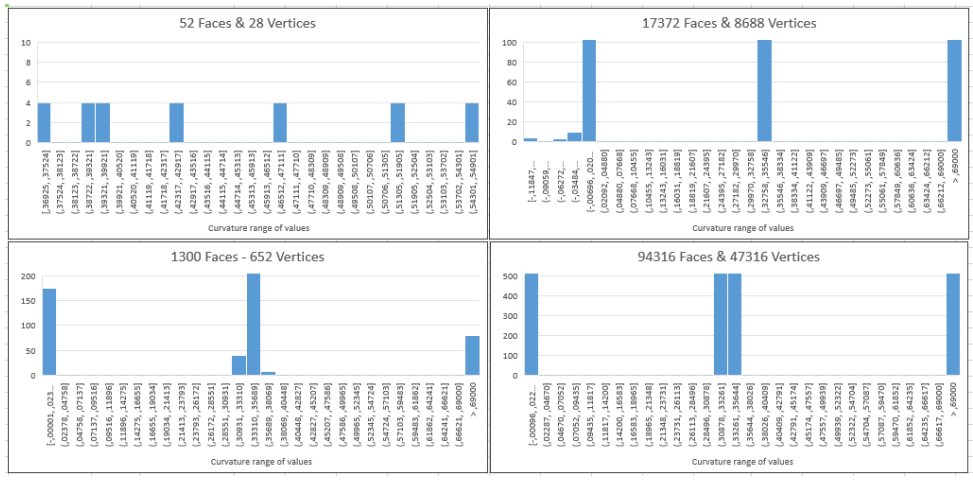

Figure 6: Histograms presenting curvature data distribution of cylinder for different triangular meshes

the impact of each rule on the final outcome. A print failure may occur because of structural problems (e.g. a collapsed wall), dimensional accuracy deviations (e.g. holes with a smaller diameter) or functionality and assembly issues (e.g. parts that must fit together, e.g. a screw). Printing problems may also arise in models

© 2021 CAD Solutions, LLC, http://www.cad-journal.net

B3 V: 8,0 cm & H: 2,5 cm & D: 8,0 cm- Volume: $9,534e-005$ m3				
Triangular Mesh No of faces	(Volume e-005)m3	Bbox (cm) X axis	Y axis	Z axis
634	9.511	8.00	2.50	8.00
6382	9.534	8.00	2.50	8.00
44984	9.534	8.00	2.50	8.00
394682	9.534	8.00	2.50	8.00

Table 3: Geometrical measurements of B3 Benchmark

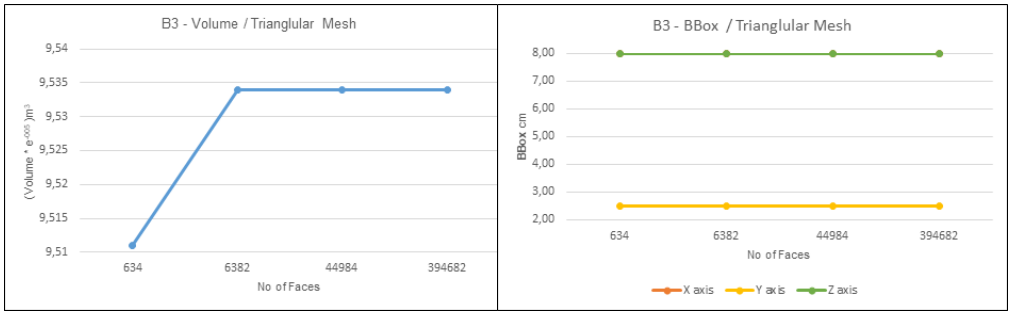

(a) Volume to Triangular mesh diagram (b) Bbox to triangular mesh diagram

Figure 7: Diagrams presenting the effect of triangular mesh over (a) B3 volume and (b) B3 bbox

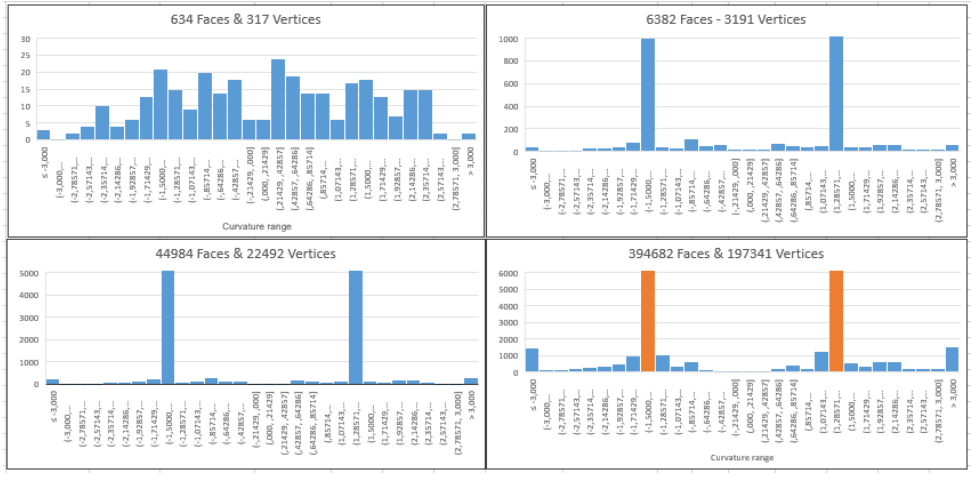

Figure 8: Histograms presenting curvature data distribution of B3 benchmark for different triangular meshes

with high level of detail on a small surface part (see e.g. filigree jewelry [14]) due to AM technology limitations. Another type of "poor printability" is encountered when many support structures must be included to facilitate printing. These supports, when removed, may lead to rough surfaces or damages to the core model.

© 2021 CAD Solutions, LLC, http://www.cad-journal.net

To this end, we propose a suite of part characteristics based on best design practices depicted in Figure 9. More specifically, there are design rules that, when applied, ensure the structural robustness of the model. Part characteristics that fall into this category are walls (supported, unsupported, minimum wall thickness), holes (minimum diameter), pins (min diameter), Boolean operation parameters (e.g. overlapping components unioned to form a larger one) and overhangs. These part characteristics must conform with size limitations that are derived from the manufacturing accuracy of various AM technologies to ensure printability. Design parameters are also defined for achieving distinct level of detail for parts that are embossed or engraved, i.e. text reliefs on a manufactured part. There are design guidelines that pertain to support construction, which mainly concerns a subset of AM technologies. Supports should be added in the case of overhangs and bridges (for some AM machines) for the model to be printable. Support construction on its own adds complexity to the printing process in terms of cost and post processing labor. Lastly, there are design rules that refer to tolerance and dimensional accuracy issues and practices that ensure the functionality of connected and/or moving parts. In this work we shall provide examples of characterizing 3D printability by translating such rules and practices with respect to the FDM, 3DP and Polyjet 3D printing technologies. Our framework can be used to characterize printability in other AM technologies as well by tuning model parameters.

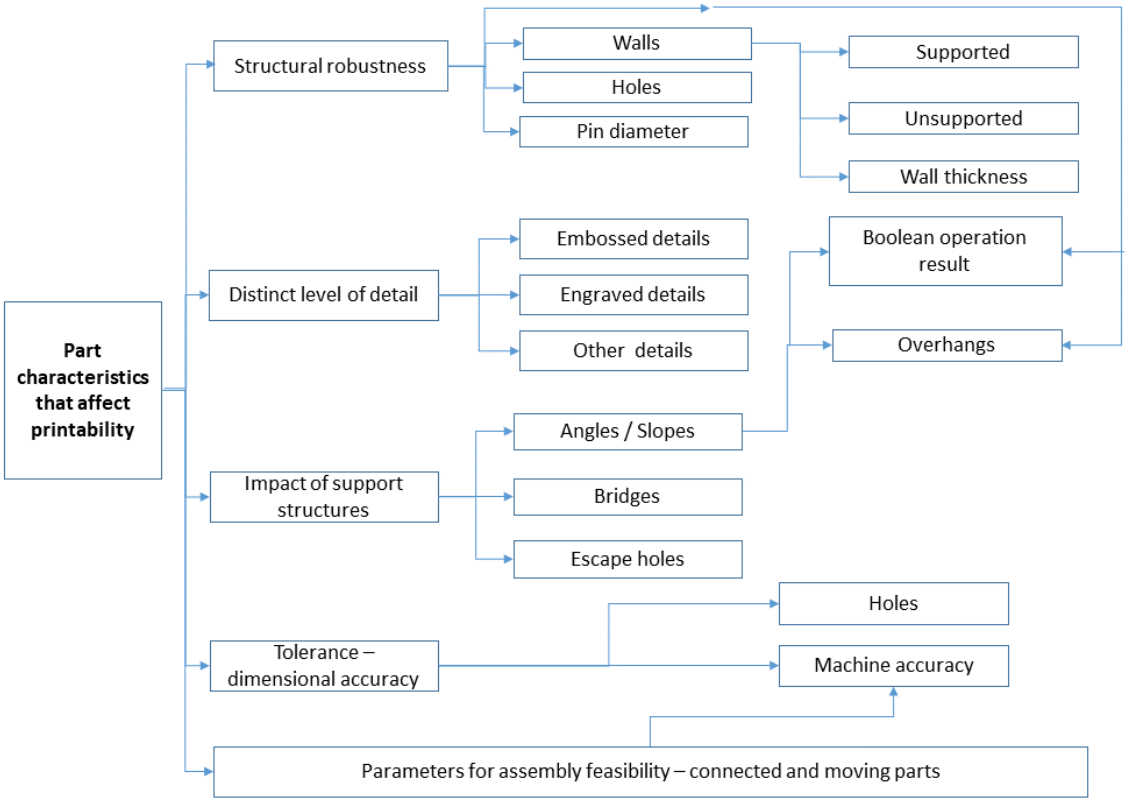

Figure 9: Design characteristics

© 2021 CAD Solutions, LLC, http://www.cad-journal.net

4 A CHARACTERIZATION OF 3D PRINTABILITY

In this work we define a measure that characterizes the printability P of a model M on a 3D printing technology T. This printability score is expressed by a number on a scale of 0 to 100, where 0 is a model that will result in a print failure on a specific printing technology and 100 corresponds to a model that is structurally robust and flawless when printed using a specific AM technology. The printability score is defined by two factors: the global probability function and the part characteristic probability function.

The global probability function expresses the probability of printing problems due to the printing characteristics of the AM machine to be employed and the model mesh complexity. If $P_G(C_M, T)$ is the global probability function for printing problems on a technology T, based on the mesh complexity C_M of the model and the technology used, then $(1-P_G(C_M, T))$ is the corresponding probability function for a successful print.

A meshed model *M* can also be described by a set of part characteristics i, that affect the printability of the model. If $P_F(i, D, T, A)$ is the probability of a part characteristic i with a set of characteristic parameters D to exhibit a flaw regarding an application A that will affect the entire printed model for a specific printing technology T, then $(1 - P_F(i, D, T, A))$ is the probability of the part characteristic to lead to a successful overall printing result. The overall probability of a model M to be successfully printed on technology T is:

$$P(M,T) = (1 - P_G(C_M,T)) * \prod_{1}^{n}(1 - P_F(i,D,T,A)) \tag{3}$$

Then the printability measure (score) of M on T is:

$$PS(M,T) = 100 * P(M,T) \tag{4}$$

4.1 Global Probability Function

The global probability function is related to the machine characteristics of the technology employed for printing. Objectively each technology has advantages and disadvantages [11]. A selection of technology characteristics that were deemed as very significant was made and is summarized in Table 4. An initial quality score $QS_T(h)$ was assigned to each characteristic h based on the technical specifications of each technology T and on the literature. Next, the quality score was transformed into probability values as shown in Table 5. For example, a *** quality score for a characteristic means that is will hardly, if at all, have a negative effect on the printing process. Therefore a very small print fail probability value will be assigned to this characteristic, e.g. 0.1, whereas a lower quality score of * means that this characteristic of the technology affects the overall print quality of the model and as such is assigned a higher print penalty, such as 0.9.

Characteristic	FDM	Binder Jetting	Material Jetting
Accuracy	**	**	***
Surface Texture	*	**	***
Various Abnormalities (Warping, shrinkage etc.)	*	**	***
Support Construction	**	***	**

Table 4: Selection and scoring of printing technologies: ***=best quality, **=average quality, *=lower quality

The quality score QS_T of a specific technology T corresponds to the product of the quality score of each

© 2021 CAD Solutions, LLC, http://www.cad-journal.net

Quality Scoring	***	**	*
Probability for characteristic to negatively effect printing	0.1	0.5	0.9

Table 5: Relating the quality score to a negative printing effect

of $m = 4$ selected characteristics (Equation 5).

$$QS_T = \prod_{h=1}^{m} QS_T(h) \tag{5}$$

For example, in the case of FDM and the Tables 4 and 5:

$$\begin{aligned} QS_{FDM} =& QS_{FDM}(Accuracy) * QS_{FDM}(SurfTex) * QS_{FDM}(Abnormalities) * QS_{FDM}(SuppConst) \\ =& 0.5 * 0.5 * 0.9 * 0.9 = 0.2025 \end{aligned} \tag{6}$$

Respectively, the quality scores for the other technologies are $QS_{BJ} = 0.0125$ and $QS_{MJ} = 0.0005$.

The aforementioned evaluated overall quality score for the 3D printing characteristics of the technology chosen provides an initial characterization of its quality ranking.The values chosen for the scoring schema can be altered depending on the requirements and restrictions desired for determining printability. For an application with strict requirements, more harsh and severe penalty values could be used, in contrast to an application that favors printability of a lower quality. Also, this process could be adopted and adapted for other 3D printing technologies. In the scope of this work, we propose penalty values that apply to applications that demand printability of a relatively high standard, for three common and representative AM technologies. Also, the character selection schema is flexible: more/other characteristics of a printing technology may be chosen and integrated into the proposed schema.

The other factor that determines the global probability function of a model on a specific technology is mesh complexity. Models of low mesh complexity produce parts of lower quality whereas meshes of higher complexity lead to products of a much better quality and robustness. Therefore, we assign a quality score QS_{C_M} to the model based on the ratio of the mesh surface area A_M and the surface area A_O of the original CAD model. This ratio expresses the probability of a satisfactory printing result due to mesh resolution(7).

$$QS_{C_M} = A_M / A_O \tag{7}$$

Therefore, the probability of an inadequate printing result is expressed by $1 - QS_{C_M}$, and as such the the global probability function of a model M is evaluated by Equation 8:

$$P_G(C_M, T) = k * QS_T * (1 - QS_{C_M}) \tag{8}$$

where k is a constant ($k > 0$) that changes the sensitivity of the global probability function, intensifies or reduces its overall contribution to the printability score.

Example: Given the CAD model of a sphere (diameter 30mm) and four different mesh representations (STL files of different resolutions), the global probability function for each model is computed on the three AM technologies, based on the information in Tables 4 and 5. The results are depicted in Table 6. For k=10, the model with the lowest mesh complexity (168 triangles) is presented with a slightly lower probability function than the more dense meshes, especially on FDM technology. However, for a higher value of k, this difference in the mesh complexity is more significant, evidently affecting the global probability function values. For $k = 0$, $P_G(C_M, T) = 1$.

© 2021 CAD Solutions, LLC, http://www.cad-journal.net

C_M	FDM	Binder Jetting	Material Jetting	FDM	Binder Jetting	Material Jetting
168	0.9159625	0.9948125	0.9997925	0.78990625	0.98703125	0.99948125
1520	0.98947	0.99935	0.999974	0.973675	0.998375	0.999935
14640	0.998785	0.999925	0.999997	0.9969625	0.9998125	0.9999925
148224	0.9998785	0.9999925	0.9999997	0.99969625	0.99998125	0.99999925

Table 6: Global probability function values for mesh models of a sphere with 168, 1520, 14640 and 148,224 triangles (left) with k=10 and (right) k=20

4.2 Part Characteristic Probability Function

For each design part characteristic i we determine a part characteristic probability function (PCP function) P_F that depends on the printing technology T, the design characteristic i and the application A. A part characteristic i that falls under the categorization depicted in Figure 9 is susceptible to flaws occurring for each design rule that is violated (since this increases the probability of a print failure). To determine the flaw probability function P_F of a part characteristic we consider the following parameters: (i) The weight $w(T,i) \geq 0$ is a numerical parameter that depends on the technology and the design characteristic, and is the dimension value of the design characteristic i that has probability 0.5 to exhibit a significant flaw during printing on technology T. This parameter can be determined by the thresholds reported by [4]. (ii) The significance $0 < s(A,i) \leq 1$ expresses the impact of the corresponding design characteristic i on the printed model regarding application A.

The PCP function of a part characteristic that corresponds to thin parts or small holes can be described by Equation 9:

$$P_F(i,d,T,A) = (1 - \frac{1}{1+e^{w(T,i)-d}}) * s(A,i) \tag{9}$$

where i is the characteristic under evaluation, d is its dimension (for holes and thin parts), $w(T,i)$ and $s(A,i)$ are the two numerical parameters described above.

For example a model with a printability score of less than 70 has a high chance of exhibiting structural robustness problems and/or undesired characteristics (i.e. warping, rough surfaces). The strict threshold under which a model will be characterized as 'unprintable' can be defined by the needs of the end-user.

PCP functions for other characteristics can be derived using the approach presented in this section. An additional factor that should be used for support characteristics is the ratio of the surface of the model affected by support structures over the entire model surface area.

5 VALIDATION OF THE PRINTABILITY MEASURE THROUGH TEST CASES

The evaluation of our proposed scoring method was performed using three AM machines using different technologies: FDM, 3DP and Polyjet. The FDM 3D printer used in this study is the Ultimaker 3 Extended. Its dimensional accuracy is $0.2 - 0.02\,mm$ for a $0.4mm$ nozzle and it was used with Polylactic Acid (PLA) filament as a feedstock material. The 3DP, Binder Jetting technology based AM machine used in our research is the ZCorp 450 3D printer and its dimensional accuracy is $+/-0.102mm$. We have also tested our models on the Stratasys Connex3 Objet 260, representing Polyjet technology, and having a dimensional accuracy of Up to $200\,microns(0.2mm)$.

The test models used for evaluation were geometric primitives and the three benchmark models (see Section 3). Each geometric primitive was printed 5 times on each AM machine and each benchmark was

© 2021 CAD Solutions, LLC, http://www.cad-journal.net

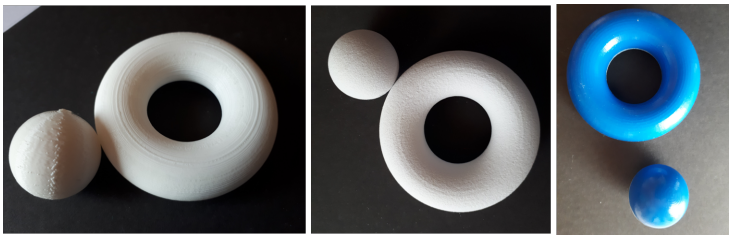

Figure 10: Examples of printed primitives on FDM, 3DP and Polyjet

printed 3 times. Sample photos of the tori and spheres printed on the three AM machines are displayed in Figure 10. The printability score for each model on each technology was calculated before printing (Table 7), having $k = 15$ for the global probability function. We evaluated the printability scores tuning the parameters such that a high sensitivity was set for holes and thin parts. The geometric primitives do not contain any part characteristics that may lead to a print failure, therefore their part characteristic probability functions are equal to 0. Given this, their printability scores are derived only from their global probability functions. Based on the printability scores, the sphere on FDM technology has a higher probability to display printing errors. Also, the cylinder, rectangular parallelepiped and torus have a top printability score of 100% on Polyjet technology, while the cylinder and the rectangular parallelepiped also score the same on 3DP. As for the printability scores of the benchmark models, the part characteristic probability functions are evaluated for thin walls and holes.

	Printability Score ($k = 15$)		
Model	FDM	Binder Jetting	Material Jetting
Sphere	99.67%	99.98%	99.99%
Cylinder	99.96%	100%	100%
Torus	99.96%	99.999%	100%
Rect. Parallelep.	100%	100%	100%
B1	26.38%	24.29%	33.50%
B2	58.18%	33.64%	57.39%
B3	76.77%	49.99%	73.09%

Table 7: Printability score of printed models

After printing and post processing, we evaluated the fabricated parts from different perspectives: dimensional accuracy, structural robustness and surface quality.

To evaluate the dimensional accuracy of all the fabricated parts and the overall conformity to the original models, we performed measurements with a digital caliper, obtaining at least 10 measurements for each dimension. These measurements were then processed to calculate the mean value for each dimension. With these values we calculated the deviation in reference to the dimensions of the original mesh model that was used for fabrication. In general, the parts fabricated using Polyjet technology were more accurate and displayed repeatability and consistency, in contrast to the other technologies. For example, when measuring the sphere, measurements we obtained from both the XY axis and the Z axis. The results for the sphere are displayed in Figure 11. The parts printed with Polyjet technology where the most accurate in both XY and Z. The 3DP parts were smaller than the original on the XY axis, which could be explained by the lower resolution of the

© 2021 CAD Solutions, LLC, http://www.cad-journal.net

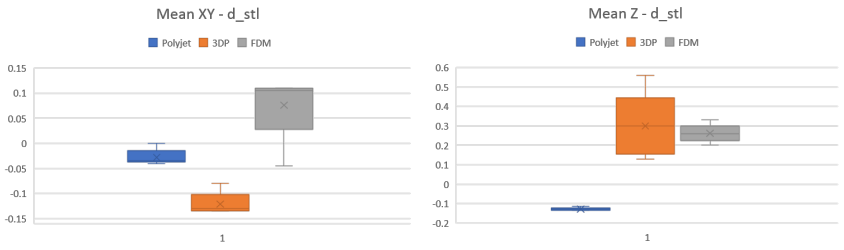

Figure 11: Display of XY deviation from original sphere mesh

machine on XY, whereas on the Z axis they were larger. The parts printed on FDM were generally larger in both directions. Also, a characteristic of the FDM parts was that they displayed warping. For example, when evaluating the diameter of the cylinder, a distinct differences were recorded throughout its length.

For the geometric primitives we calculated the ratio l of the volume of the fabricated part A, V_A, to the volume of the initial mesh model M,V_M, to measure the actual accuracy of the AM machine (Equation 10). In general, the objects that were printed on Binder Jetting technology had the smallest deviation in volume size from the original model.

$$l = \frac{V_M}{V_A} \tag{10}$$

	Ratio $l = V_M/V_A$		
Sphere-1	Polyjet	3DP	FDM
Sphere-2	0.993682194	1.010465886	1.021082769
Sphere-3	0.993433109	1.001674907	1.017535587
Sphere-4	0.993433109	1.026164459	1.012230231
Sphere-5	0.993682194	1.004181391	1.023875618

Table 8: Volume ratios of printed sphere models

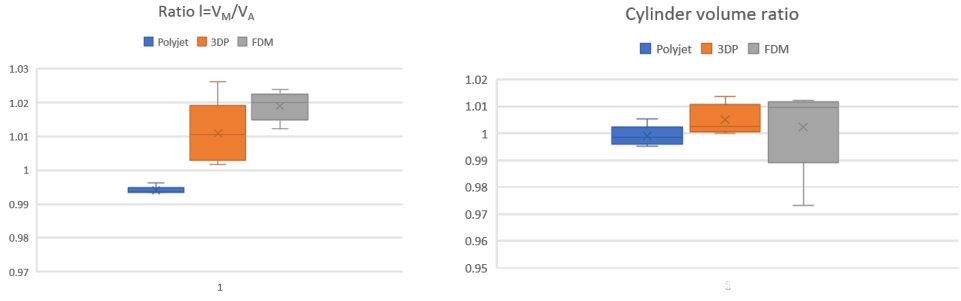

(a) Sphere volume ratio

(b) Cylinder volume ratio

Figure 12: Comparison of the volume ratios for the parts fabricated on the three technologies

© 2021 CAD Solutions, LLC, http://www.cad-journal.net

In reference to the structural robustness of the fabricated parts, no issues were found in the geometric primitives. In benchmark B1, there were structural problems in some models. In the FDM prints, the thinnest bridges could not be cleaned of the supports; there was a structural collapse when this was attempted. The same problem arose in 2 of the 3 Polyjet parts. In the 3DP model, the thin bridges were printed, however they broke in post processing. In all model the holes were printed, however in the FDM parts some holes were not circular. As for benchmark B2, the overhangs with the 2 smallest angles were not printed well on FDM, and in the 3DP models there was a print failure whilst cleaning. The 2 thinnest walls couldn't be printed successfully on FDM, and on 3DP the thinnest broke in one of the three models, while the other two presented warping (13).

As for the structural texture and aesthetic result, there is distinct difference in quality. The FDM parts are rough, with more surface anomalies, hairs, uneven surfaces from material deposition. 3DP parts are slightly porous but with a better level of detail and no anomalies due to lack of supports. The polyjet prints have a very smooth surface with good level of detail.

Given the above observations, we reviewed the printability scores of the models. In reference to the geometric primitives (Figure 10), the printing scores conform with the result: all four primitives are printable, without features that can cause a structural failure. The difference in printability scores on all technologies for a model, e.g. the sphere, is justified, through the measurements but also visually, as shown in Figure 10. The sphere printed on the FDM machine has surface abnormalities that are not present in the other parts.

As for the benchmark models, B1 had a printability score that was low and this is justified by the fact that there was breakage of thin parts on all AM machines. Model B2 had a higher printability score than B1, but still relatively low, and this proved correct since there were print failures of thin walls. The printability score of B3 was much better, and therefore the model was robustly printed on all technologies.

In Figures 13 and 14 we showcase a few examples of models that have been used in this process.

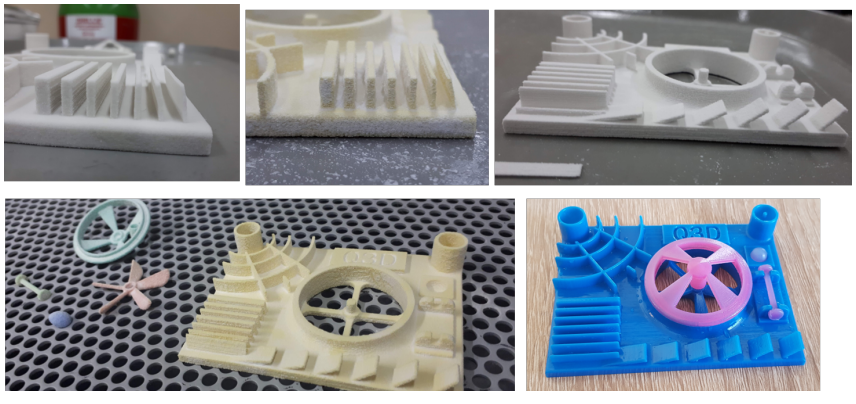

Figure 13: 3DP and FDM prints of the B2 benchmark

6 CONCLUSIONS

In this paper we have proposed a novel approach to characterizing the efficacy of manufacturing a designed CAD model on an AM machine of a certain technology, based on its model complexity and part characteristics. These elements are mapped to parameters and functions, that depend also on the printing technology to be employed, that make up a linear formula that corresponds to a *printability* score. This measure, which is evaluated using worst case printing scenarios, can be used either to determine which 3D technology is more

© 2021 CAD Solutions, LLC, http://www.cad-journal.net

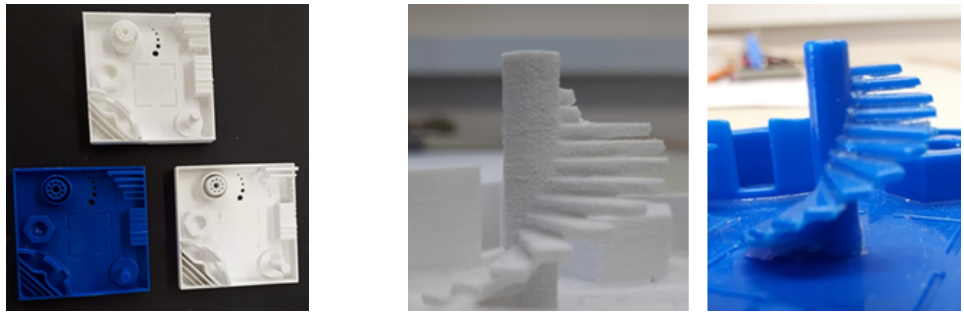

(a) FDM(top), Polyjet(b.left) & 3DP(b.right) (b) Staircase printed on 3DP and Polyjet

Figure 14: The printed B1 benchmark model on three different technologies

suitable for manufacturing a specific model or can be used as a guide to redesigning the model so that it is more suitable for an intended specific technology.

As future work we intend to evaluate more part characteristics and their impact on printability. We will evaluate the volume ratios of the benchmark models with methods of photogrammetry and laser scanning to further validate our approach. Also our proposed printing score system can be adapted to include other AM printing technologies and other design intents.

ACKNOWLEDGEMENTS

This research has been co-financed by the European Union and Greek national funds through the Operational Program Competitiveness, Entrepreneurship and Innovation, under the call RESEARCH -CREATE -INNOVATE (project code:T1EDK– 04928)

ORCID

Ioannis Fudos http://orcid.org/000-0002-4137-0986
Margarita Ntousia http://orcid.org/0000-0003-4615-4569
Vasiliki Stamati http://orcid.org/000-0002-4225-3685
Paschalis Charalampous http://orcid.org/0000-0002-9399-4387
Theodora Kontodina http://orcid.org/0000-0002-8534-1722
Ioannis Kostavelis http://orcid.org/0000-0003-2882-2914
Dimitrios Tzovaras http://orcid.org/0000-0001-6915-6722
Leonardo Bilalis http://orcid.org/0000-0003-2343-9385

REFERENCES

[1] Abshire, M.: 3D CAD design for 3D printing tips, tricks, & techniques part 1 of 3. https://www.cati.com/blog/2018/05/3d-cad-design-3d-printing-tips-tricks-techniques-part-1//.

[2] Adam, G.; Zimmer, D.: On design for additive manufacturing: evaluating geometrical limitations. Rapid Prototyping Journal, 21(6), 662–670, 2015. http://doi.org/https://doi.org/10.1108/RPJ-06-2013-0060.

[3] Booth, J.; Alperovich, J.; Chawla, P.; Ma, J.; Reid, T.; Ramani, K.: The design for additive manufacturing worksheet. Journal of Mechanical Design, 139, 2017. http://doi.org/10.1115/1.4037251.

© 2021 CAD Solutions, LLC, http://www.cad-journal.net

[4] Brockotter, R.: Key design considerations for 3d printing. https://www.3dhubs.com/knowledge-base/key-design-considerations-3d-printing/.

[5] Gibson, I.; Rosen, D.; Stucker, B.: Additive Manufacturing Technologies. Springer-Verlag New York, January 2015, 2015. ISBN 978-1-4939-2112-6, 978-1-4939-2113-3, 978-1-4939-4455-2. http://doi.org/10.1007/978-1-4939-2113-3.

[6] Globa, D.M., A.A.; Ulchitskiy, O.: Metrics for measuring complexity of geometric models. Scientific visualization, 8(5), 74–82, 2016.

[7] Jee, H.; Lu, Y.; Witherell, P.: Design rules with modularity for additive manufacturing. Proceedings of the Solid Freeform Fabrication Symposium, 2015.

[8] Kim, H.; Lin, Y.; Tseng, B.: A review on quality control in additive manufacturing. Rapid Prototyping Journal, 24, 645–669, 2018. http://doi.org/10.1108/RPJ-03-2017-0048.

[9] Mani, M.; Witherell, P.; Jee, H.: Design rules for additive manufacturing: A categorization. 1–10. ASME 2017 International Design Engineering Technical Conferences and Computers and Information in Engineering Conference, 2017. http://doi.org/10.1115/DETC2017-68446.

[10] Michael D. Johnson, L.M.V.; Thomison, W.D.: An investigation and evaluation of computer-aided design model complexity metrics. Computer-Aided Design and Applications, 15(1), 61–75, 2018. http://doi.org/10.1080/16864360.2017.1353729.

[11] Ntousia, M.; Fudos, I.: 3D printing technologies and applications: An overview. 243–248. Proceedings of the CAD Conference in Singapore, 2019. http://doi.org/10.14733/cadconfP.2019.243-248.

[12] Oropallo, W.; Piegl, L.A.: Ten challenges in 3d printing. Engineering with Computers, 32(1), 135–148, 2016. ISSN 0177-0667. http://doi.org/10.1007/s00366-015-0407-0.

[13] Rossignac, J.: Shape complexity. Visual Computer, 21, 985–996, 2005. http://doi.org/10.1007/s00371-005-60362-7.

[14] Stamati, V.; Antonopoulos, G.; Azariadis, P.; Fudos, I.: A parametric feature-based approach to reconstructing traditional filigree jewelry. Computer Aided Design, 43(12), 1814-1828, 2011. ISSN 0010-4485. http://doi.org/10.1016/j.cad.2011.07.002.

[15] Tofail, S.A.; Koumoulos, E.P.; Bandyopadhyay, A.; Bose, S.; O'Donoghue, L.; Charitidis, C.: Additive manufacturing: scientific and technological challenges, market uptake and opportunities. Materials Today, 21(1), 22–37, 2018. ISSN 1369-7021. http://doi.org/https://doi.org/10.1016/j.mattod.2017.07.001.

[16] Tompson, M.; Moroni, G.; Vaneker, T.; Fadel, G.; Campbell, I.; Gibson, I.; Bernard, A.; Schulz, J.; Graf, P.; Ahuja, B.; Martina, F.: Design for additive manufacturing: Trends, opportunities, considerations, and constraints. CIRP annals : manufacturing technology, 65(2), 737–760, 2016. ISSN 0007-8506. http://doi.org/10.1016/j.cirp.2016.05.004.

[17] Yang, S.; Zhao, Y.F.: Additive manufacturing-enabled design theory and methodology: a critical review. The International Journal of Advanced Manufacturing Technology, 80(1), 327–342, 2015. ISSN 1433-3015. http://doi.org/10.1007/s00170-015-6994-5.

[18] Zhang, Y.; Bernard, A.; Gupta, R.; Harik, R.: Feature based building orientation optimization for additive manufacturing. Rapid Prototyping Journal, 22(2), 358–376, 2016. http://doi.org/https://doi.org/10.1108/RPJ-03-2014-0037.

© 2021 CAD Solutions, LLC, http://www.cad-journal.net